Est. 1984

ORIENTAL JOURNAL OF CHEMISTRY

An International Open Access, Peer Reviewed Research Journal

www.orientjchem.org

ISSN: 0970-020 X
CODEN: OJCHEG
2019, Vol. 35, No.(2):
Pg. 523-530

Potassium Gluconate inhibition of α-Brass Corrosion in 1 M HNO_3

CLEOPHAS AKINTOYE LOTO[1,2] and ROLAND TOLULOPE LOTO[1]

[1]Department of Mechanical Engineering, Covenant University, Ota, Nigeria.
[2]Department of Chemical, Metallurgical and Materials Engineering, Tshwane University of Technology, Pretoria, South Africa.
*Corresponding author E-mail: akinloto@gmail.com; cleophas.loto@covenantuniversity.edu.ng

http://dx.doi.org/10.13005/ojc/350203

(Received: November 03, 2018; Accepted: March 12, 2019)

ABSTRACT

Potassium gluconate inhibition effects of α-brass corrosion immersed in 1 M HNO_3 were studied at room temperature (25°C). Gravimetric and potentiodynamic polarization measurement techniques were used separately for the experimental investigation. A Digi-Ivy potentiostat, connected to computer for data acquisition and analyses was used for the potentiodynamic polarization experiments. The observed potassium gluconate's corrosion inhibition increased as the inhibitor concentration increased up to 3.5g/200 ml HNO_3 where a 0.7224 g weight loss was recorded in comparison with the experiment without added inhibitor which had a 3.582 g weight loss at 312 hours. The corresponding corrosion rate at 3.5g/200 ml HNO_3 concentration was 4.93 mm/yr while the uninhibited (control) experiment recorded a 20.33 mm/yr at 288 hours. Corrosion inhibition efficiency values for the 1.5, 3, 3.5 and 4g/200ml HNO_3 concentrations are respectively 16.99, 41.77, 79.86 and 64.53%. Other parameters recorded include: polarization resistance, Ω (3.20E+01); corrosion rate (19.15 mm/yr) and current density, 1.01E-03 Acm^{-2} for the 3.5g/200 ml HNO_3 concentration in HNO_3 test medium were also achieved. A mixed type inhibitor was indicated with the recorded results of ba and bc. Adsorption isotherm showed that inhibitor protection mechanism followed both the Frumkin and the Freundlich models more than the Langmuir isotherm model.

Keywords: Corrosion, Inhibition, Potassium gluconate, Polarisation, Nitric acid.

INTRODUCTION

In terms of wide use and versatility in industrial and services application, the copper – zinc alloys of which α-brass is one, are of significant importance in material's selection consideration for corrosion and protection in corrosive environments. Alpha brass has the properties that make it very attractive for use in different industrial concerns and metals' technology application. Though relatively corrosion resistant, its susceptibility in diverse environments such as in acid, water, alkaline, atmosphere and in mercury, is disadvantageous; and hence creates further interest in corrosion prevention, control and protection research[1-7]. Inhibitors have been used for alpha brass's protection. The alloy is particularly known to be susceptible to nitric acid corrosion[8-14].

In general, corrosion inhibitors are chemical compounds whose reacting species interact with the metal surface and producing a film barrier at the metal-environment interface to inhibit corrosion reactions. The mechanism of corrosion inhibition then could be either by altering the anodic or cathodic polarization behaviour, increasing the electrical protection of the metal's surface, reducing the spreading of ions to the metal surface or a combination of any of the three with another one. The influence of inhibitors is often associated with physical or chemical adsorption. This phenomenon had been associated with N, O, S, and multiple bonds or aromatic rings in the inhibitor that were available as hetero atoms[12]. These atoms could be seen more in organic compounds inhibitors. In this work, the corrosion and inhibition of alpha brass was studied. The investigation aims at studying the inhibition effect of potassium gluconate on the corrosion resistance of α-brass in nitric acid medium. Potassium gluconate has the formula $C_6H_{11}KO_7$, and is also usually referred to as 2, 3, 4, 5, 6-pentahydroxycaproic acid potassium salt. It is also called D-gluconic acid potassium salt, or potassium D-gluconate[16]. Potassium gluconate could be used as a mineral supplement and sequestrant. The results obtained are expected to be of scientific, technological and economic benefits.

The chemical structure of potassium gluconate is presented below:

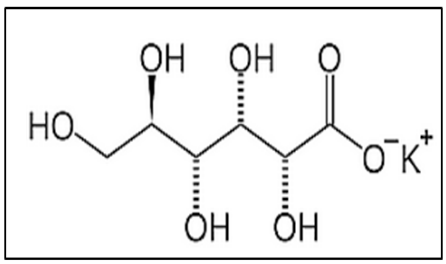

Chemical structure of potassium gluconate, $C_6H_{11}KO_7$[16]

EXPERIMENTAL

Specimens preparation

Cylindrical α-brass alloy sample was cut to 20 mm x 10 mm coupons for the experiments. The specimens were de-scaled with a wire brush and then ground with various grades of emery paper. They were subsequently polished to 6 μm and rinsed in distilled water to remove any dirt and then degreased with acetone. Samples for the polarization experiments were joined to copper wire and then mounted in araldite resin with only the surface to be tested exposed. They were further similarly polished, cleansed and degreased as described above. All the samples were protectively kept for further experiments.

Experiments for Weight loss method

Prepared specimens were separately weighed and immersed, in turns, in each of the test media contained in a beaker (250 ml) for 336 hours. For each test, two coupons were used and the average weights recorded. The test medium was 1M HNO_3. Various amounts of potassium gluconate were separately added in different beakers. Weights of potassium gluconate used ranged from 1, 1.5, 2, 2.5, 3, 3.5 to 4 g; and these were separately added to 200 ml of nitric acid. There was also the control experiment with no inhibitor addition. Results of weight-loss were recorded every 48 hours. The plots of accumulated weight loss and of corresponding calculated corrosion rate versus exposure time are respectively presented in Fig. 1 to 2. Corrosion rate, (C. R. (mm /y)) was calculated from the formula in Equation 1.

$$C.\ R. = 87.6 \times (W/DAT) \quad (1)$$

Where, W = Weight loss in milligrams; D = Metal density in g /cm^3; A = Exposed area of sample in cm^2; T = Time of exposure of the metal sample in hours.

From the corrosion rate results obtained from the experimental readings, the percentage inhibitor efficiency, P, was calculated from the equation:

$$P = 100[1-W2/W1] \quad (2)$$

W1 = the corrosion rate in the absence of the potassium gluconate inhibitor.

W2 = the corrosion rate in the presence of the predetermined concentration of the potassium gluconate inhibitor.

Surface coverage

Surface coverage can also be used to show the effectiveness of the inhibitor on the metal's

surface[17]. Surface coverage was calculated from the formula in equation 3.

$$¢ = (CR_{blank} – CR_{inh})/CR_{blank} \quad (3)$$

From the above, ¢ = surface coverage; CR_{blank} = corrosion rate without inhibitor, and CR_{inh} = the corrosion with inhibitor.[18]

Potentiodynamic polarization experiments

Potentiodynamic polarization experiments were performed with the mounted specimens in turns by immersing each one in each of the acid test media with the addition and without the addition of different amounts of inhibitor. The exposed surface of the mounted specimen (1 cm^2 surface area) was immersed in the test solution. The experiments were done using a polarization cell. It consists of a three -electrode system, that is, a reference electrode (silver chloride electrode– SCE), a working electrode (WE); and two - carbon rod counter electrodes (CE). The polarization cell was connected to potentiostat (Digi-Ivy potentiostat). A scan rate of 0.00166 V/s from –1.5 to +1.5 V was used for the potentiodynamic tests. The experiments were separately conducted with different potassium gluconate inhibitor amounts in the 1M HNO_3.

RESULTS AND DISCUSSION

Weight loss experiment

The results obtained from the experiments of the different amounts of potassium gluconate addition for α-brass corrosion in 1M HNO_3 are presented in Figure 1.

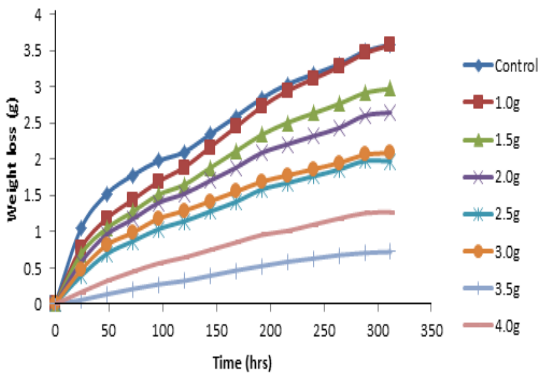

Fig. 1. Curves of weight loss of α-brass versus exposure time immersed in 1 M HNO_3 with different amounts of potassium gluconate addition

The test specimens immersed in the 1M HNO_3, without the inhibitor addition, lost the most weight (3.582 g) within thei13 days (312 h) experimental period. It recorded a 3.1751 g weight -loss at 240 h (10 days). The sample used with 1.5 g of inhibitor concentration showed some improvement in inhibition up to 250 h achieving a 3.11g weight-loss. At the end of the experiment, the 3.5 g and 4.0 g inhibitor concentrations, showed better inhibition with recorded 0.7224 g and 1.2719 g metal weight loss respectively.

Corrosion rate

Figure 2 shows the corresponding corrosion rates obtained by calculations from the weight loss results. The highest corrosion rate (92.45mm/yr) at the end of the experiment was recorded after the first day of the test without added inhibitor (control experiment). Results of corrosion rates for all the other concentrations were very close indeed. They were betweeni 24.46 to 4.93mm/y for 1.0g- to 4.0g/200 ml 1M HNO_3 inhibitor concentrations respectively. These results show the effectiveness of the potassium gluconate inhibitor concentrations on α-brass corrosion in 1M HNO_3. The 3.5g/200 ml 1M HNO_3 inhibitor concentration had the lowest recorded corrosion rate (4.93mm/y) at 288 h (12 days).

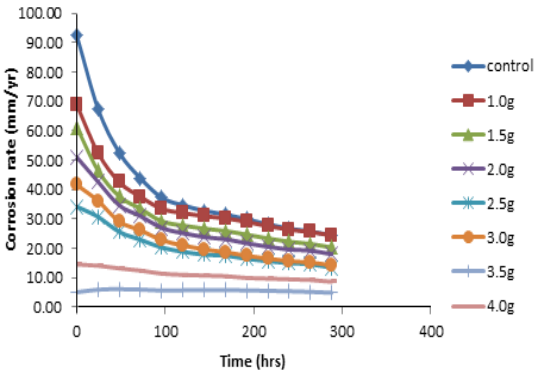

Fig. 2. Curves of corrosion rate of α-brass with exposure time in 1 M HNO3 with different concentrations of potassium gluconate inhibitor addition

Surface Coverage

Figure 3 shows the surface coverage results obtained by calculation from the inhibition efficiency. The surface coverage curves decreased with the exposure time. The test with the 3.5g/200 ml of 1M HNO_3 inhibitor concentration gave impressive surface coverage value of 0.94 at the beginning and

regressed slightly during the experiment indicating very effective protection. At 312 h, the 1 g inhibitor concentration gave lower comparative surface coverage (0.0012).

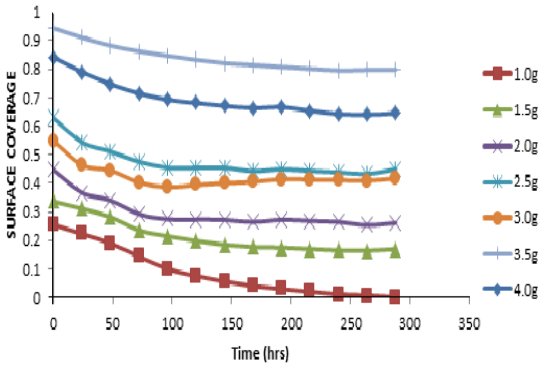

Fig. 3. Curves of surface coverage of α-brass against exposure time in 1M HNO_3 with potassium gluconate additions

Inhibition Efficiency

Figure 4 represents corrosion inhibition efficiency results of α-brass in 1M HNO_3. It could be observed that the inhibition efficiency values/graphic profile decreased with exposure time right from the high values at the beginning and achieving lower values later during the experiment. Essentially, this phenomenal observation could not be unconnected with the corrosion products in the solution causing contamination of the test environment. This consequentially rendered the environment weak and thus stifling the corrosion reactions process and reduction in corrosion rate. The potassium gluconate inhibitor concentration of 3.5g/200 ml of 1M HNO_3 had the highest percent inhibition efficiency that ranged between 94% at the beginning and 80% at the end of the experiment at 28 hours. It could thus be plausibly said that this concentration was the optimum for the inhibitor in the tested environment at the parametric conditions used in the experiment.

Results of potentiodynamic polarization experiments

Curves of Fig. 5 show the graphic results obtained for the potentiodynamic polarization experiments with and without inhibitors performed for α-brass in 1M HNO_3 test medium using different concentrations of potassium gluconate inhibitor that ranged from 1.5 to 4g/200 ml of the 1M HNO_3.

A clear observation here was that the polarization (anodic and cathodic) moved towards lower current densities whenever a change in the electrolyte concentration increase was made with the use of the inhibitor. The current densities apparently decreased for the respective increase in concentrations. The presence of O as an inhibitory substance in the inhibitor composition could provide inhibiting molecules that blocked the reaction sites on the metal's surface during the test electrode's/ HNO_3 corrosion interfacial reactions.

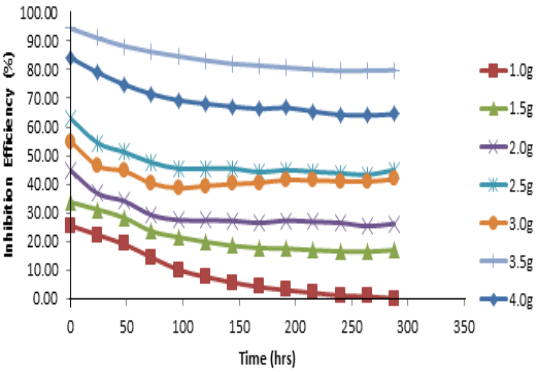

Fig. 4. Curves of inhibition efficiency of α-brass against exposure time in 1M HNO_3 using varied concentrations of potassium gluconate addition

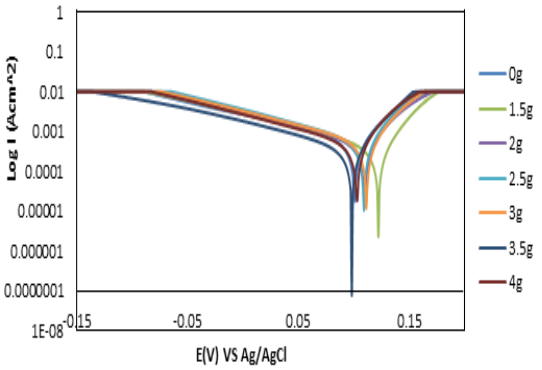

Fig. 5. Potentiodynamic polarization curves for a-brass in 1 M HNO_3

The shifting of the polarization towards more positive potentials confirmed the $C_6H_{11}KO_7$ inhibitor to have acted as a mixed inhibitor though with tilting towards anodic behaviour. With long linear stretches, the anodic side of the curves could be described to have shown Tafel behaviour which indicate that the metal oxidation was activation controlled. On the other hand, the cathodic reactions' behaviour indicates H^+ reduction process. A summary of the electrochemical corrosion polarization results

obtained during the experiments is given in Table 1. The test with 3.5g/200 ml HNO_3 potassium gluconate concentration recorded the lowest values indicated by all the experimental parameters. It recorded 0.098 V, 19.15 mm/y, 1.01E-03 A/cm^2, and 3.207E+01 Ω for the open corrosion potential, corrosion rate (CR), current density and polarization resistance respectively. The value(s) of corrosion rate continued to decrease with time. This concentration gave the best inhibition performance at the electrode/acid interface.

Table 1: Data results for potentiodynamic polarization of a-brass in HNO_3

Sample	Inhibitor Concentration (g/200 ml HNO_3)	Corrosion Rate (mm/y)	Current (A)	Current Density (A/cm^2)	Corrosion Potential (V)	Polarization Resistance (Ω)	Cathodic Tafel Slope (V/dec)	Anodic Tafel Slope (V/dec)
A	0	28.97	1.212E-03	1.53E-03	0.101	2.120E+01	-5.830E+00	6.27E-01
B	1.5	21.34	8.927E-04	1.13E-03	0.122	2.878E+01	-6.896E+00	0.000E+00
C	2	27.59	1.15E-03	1.46E-03	0.110	2.227E+01	-7.009E+00	4.117E-16
D	2.5	31.44	1.32E-03	1.66E-03	0.109	1.954E+01	-7.593E+00	4.117E-16
E	3	29.62	1.239E-03	1.57E-03	0.111	2.073E+01	-7.105E+00	0.000E+00
F	3.5	19.15	8.011E-04	1.01E-03	0.098	3.207E+01	-7.098E+00	4.117E-16
G	4	27.90	1.17E-03	1.48E-03	0.103	2.20E+01	-7.386E+00	0.000E+00

Optical microscopy examination micrographs

The representative micrographs of the α-brass test samples surfaces used in this experiment are shown in Fig. 6. In sample B which represents the specimen immersed in 1M nitric acid without added inhibitor, it could be observed that the metal's surface had been corrosively degraded by the acid. The major corrosion reacting species in this nitric acid is the NO_3^-. This polyatomic ion has the capability of penetrating metal's surface film to initiate corrosion reactions process.

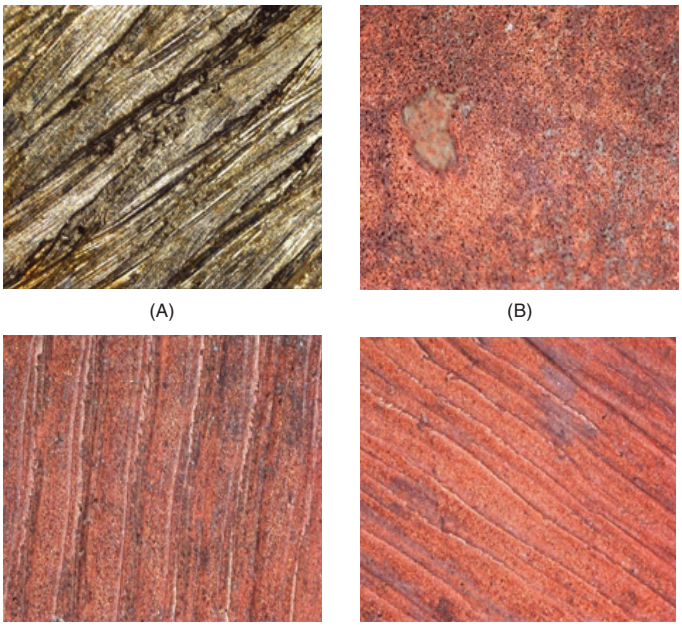

Fig. 6. Optical examination photomicrographs of α-brass before and after immersion with and without potassium gluconate addition

A. Optical micrograph of α-brass before corrosion,
B. Optical micrograph of brass in 1M HNO_3 without inhibitor addition (control),
C. Optical micrograph of brass in 1M HNO_3 + 3.5 g inhibitor conc.,
D. Optical micrograph of brass in 1M HNO_3 + 4.0 g

Inhibitor concentration

With the addition of $C_6H_{11}KO_7$ inhibitor, the metal's surface film became more stabilized by

atomic adsorption of O and OH atoms/molecules to the reacting sites on the surface and thereby reducing and/or minimizing or stops the metal's surface/nitric acid interfacial reaction(s). This was demonstrated by the 3.5 g/200 ml HNO_3 inhibitor concentration which seemed to be the optimum concentration in this experiment. The micrograph for this observation is presented in Fig. 6, sample C.

The surface integrity manifested by the crystalline structure shows that over 312 h, the 3.5 g inhibition concentration has corroded the least when compared with other samples in various concentrations. The result is in agreement with gravimetric and polarisation experimental results.

Adsorption isotherm

The process of adsorption is studied through the use of graphical models known as adsorption isotherm. $C_6H_{11}KO_7$'s adsorption to the α-brass surface is a chemical reaction involving the transfer of atoms which results in the entire coverage of the surface of the specimen. However, due to the significant differences in the metallurgical properties of the brass samples, the adsorption mechanisms will vary differently from one another. Various adsorption isotherm models was used to study the surface adsorption mechanism.

In this investigation, the phenomena of $C_6H_{11}KO_7$ inhibition could be explained by molecular adsorption to the metal electrode's surface. A number of factors that include: the nature and surface charge of metal, the type of aggressive media, the distribution of charge in molecule and the chemical structures of organic compounds Molecular adsorption process could be influenced by some factors such as the test medium reactive intensity, molecular distribution of charges and the structural chemistry of the organic compound where applicable[19]. Based on the obtained experimental results, with several adsorption isotherms, the likely mode of adsorption could be determined. The value of the adsorption equilibrium constant, k, and the standard free energy of adsorption[20] could be determined by Equation (4) below:

$$k = \frac{1}{55.5}\exp\left(-\frac{\Delta G^{o}_{ads}}{RT}\right) \quad (4)$$

Where ΔG^{o}_{ads} = the standard free energy of adsorption;

R = the molar gas constant and T is the absolute temperature.

The negative values of ΔG^{o}_{ads} obtained indicates the spontaneous adsorption process and the stability of the adsorbed inhibitor layer on the metal surface.

In this investigative report, three models were made; these are: (i) Langmuir (ii) Frumkin and (iii) Freundlich isotherms. The ΔG^{o}_{ads} for castor bark powder had been determined to be -16.92 kJ/mol[21]; and this indicates the physiosorption mode of adsorption. Values of ΔG^{o}_{ads} that are -20 kJ/mol and above, had been associated with physical adsorption (physiosorption) while those around -40 kJ/mol and more negative are generally associated with chemical adsorption. Here, Frumkin and Freundlich adsorption isotherms gave better conformance Freundlich adsorption isotherm is determined by Equations (5) and (6) below[22]

$$\theta = KC^{n} \quad (5)$$

$$\text{Log } \theta = n \text{ Log } C + \ln K \quad (6)$$

- where θ = the degree of surface coverage; K and n are coefficients; the inhibitor concentration = C. As presented in Fig. 7, a linear regression value of 0.88 was obtained when the graph of Log C was plotted with Log θ . The adsorption isotherm showed that the inhibitor protection mechanism followed both the Frumkin and the Freundlich models more than the Langmuir isotherm model.

Calculated results show the POTM perfectly aligns with the Frumkin and Freundlich adsorption isotherm in HNO_3 solution. The other adsorption isotherm model tested (Langmuir) and they gave a correlation coefficient values less than 0.8 (0.516).

Thermodynamics of the corrosion process

Table 3: Data for Gibb's free energy, surface coverage and equilibrium constant of adsorption for POTM in 1M HNO_3.

Results of Gibbs free energy values (ΔG) calculated from Equations (7) and (4) calculated from the Langmuir equation are shown in Table 3.

$$\Delta G_{ads} = -2.303RT \log [55.5K_{ads}] \quad (7)$$

Table 2: Adsorption isotherm data for α-brass in 1M of HNO_3

MCS Samples	Weight Loss (g)	POTM Concn (g/200 ml 1M HNO_3)	POTM Concentration (Molarity)	Corrosion Rate (mm/yr)	POTM Inhibition Efficiency (%)	Surface Coverage (θ)
0	3.586	0	0	24.49	0	0
1	3.582	1.0	1.07E-02	24.51	0.12	0.0012
2	2.977	1.5	1.60E-02	20.33	16.99	0.1699
3	2.647	2.0	2.13E-02	18.07	26.19	0.2619
4	1.973	2.5	2.67E-02	13.47	44.98	0.4498
5	2.088	3.0	3.20E-02	14.26	41.77	0.4177
6	0.722	3.5	3.74E-02	4.93	79.86	0.7986
7	1.272	4.0	4.27E-02	8.68	64.53	0.6453

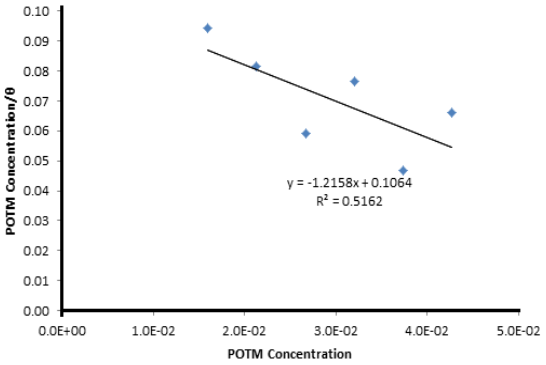

Fig. 7. Langmuir isotherm plot for the adsorption of potassium gluconate on α-brass in 1M of HNO_3

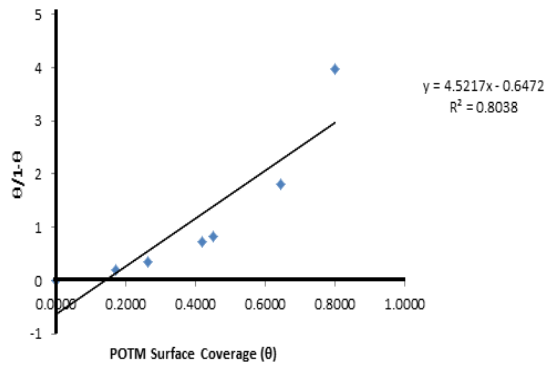

Fig. 8. Frumkin isotherm plot for POTM in 1M of HNO_3

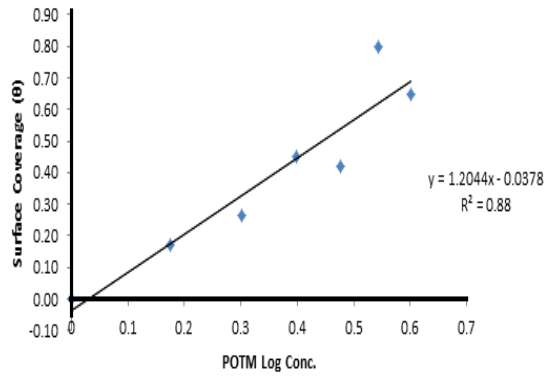

Fig. 9. Freundlich isotherm plot for POTM in 1M of HNO_3

Table 3: Data for Gibb's free energy, surface coverage and equilibrium constant of adsorption for POTM in 1M HNO_3

MCS Samples	POTM Concentration (Molarity)	Surface Coverage (θ)	Equilibrium Constant of adsorption (K)	Gibbs Free Energy, ΔG ($Kjmol^{-1}$)
0	0	0	0	0
1	1.07E-02	0.0012	112.6	-21.66
2	1.60E-02	0.1699	12787.7	-33.39
3	2.13E-02	0.2619	16626.9	-34.04
4	2.67E-02	0.4498	30643.7	-35.55
5	3.20E-02	0.4177	22404.1	-34.77
6	3.74E-02	0.7986	106127.3	-38.63
7	4.27E-02	0.6453	42621.4	-36.37

55.5 is the molar concentration of water in the solution, *R* is the universal gas constant, *T* is the absolute temperature. The ΔG values show the adsorption of POTM onto the steel during the corrosion inhibition is concentration dependent. At 1.07 x 10^{-2} M, the inhibition mode is through physisorption due to insufficient inhibitor molecules to counteract the electrochemical action of the corrosive species. This is proven from the low surface coverage value of 0.0012. Increase in POTM concentration from 1.60 x 10^2 M to 3.20 x 10^2 M had limited effect on the effective performance of corrosion inhibition properties of POTM. However, at these concentrations strong electrochemical interaction occurred between the POTM molecule and the steel surface with ΔG values between 33.39 $Kjmol^{-1}$ and 34.77 $Kjmol^{-1}$. The results are associated with chemisorption reaction mechanism i.e. reactions through electrostatic attraction and covalent bonding. At 3.74 x 10^2 M and 4.27 x 10^2 M further increase in ΔG values was observed coupled with a corresponding increase in surface coverage value associated with effective corrosion inhibition. The inhibition performance at the concentrations shows enough POTM molecules effectively substitutes H_2O molecules. This electrochemical action limits the oxidation reactions on the steel surface.

CONCLUSION

Results obtained from all tests confirmed the potassium gluconate's good inhibition for α-brass in 1M HNO_3. There was better corrosion inhibition performance for all the results parameters when the inhibitor's concentration was increased. The 3.5 g potassium gluconate concentration gave the best corrosion inhibition performance. The reaction of potassium gluconate with nitric acid provides a stable film and complex chemical compound that contributed to the passivation of the α-brass surface to stifle the corrosion process interfacial reactions. A mixed type inhibitor was indicated with the results of ba and bc. From the adsorption isotherm results, inhibitor protection mechanism was more of Frumkin and Freundlich models than the Langmuir isotherm model.

ACKNOWLEDGEMENT

The authors acknowledge the Department of Mechanical Engineering, Covenant University, Ota, Nigeria for the provision of research facilities and also the laboratory experimental work contribution of Abighe Eviano Odomero.

REFERENCES

1. Carvalho, M.L. Anal. Chem. Université Pierre et Marie Curie - Paris VI, 2014. English. <NNT: 2014PA066304>.
2. Hosseinpour, S.; Forslund, M.; Magnus Johnson, C.; Pan, J.; Leygraf, C. *Surf. Sci.*, **2016**, *648*(6), 170-176. https:// doi. org/ 10.10 1 6/j.susc. 2015.10.045.
3. Lynes, W. *Corrosion.*, **1965**, *21*(4), 125-131. https://doi.org/10.5006/0010-9312-21.4.125
4. Loto, C.A.; Loto, R.T.; Oshugbunu, O. *Mor. J. Chem.*, **2016**, *4*(3),711-721.
5. Loto, C.A. *Alexand. Eng. J.* **2018**, *57*(1), 483-490 http://dx. doi. org/ 10. 1016/j. aej. 2016. 1 2.012.
6. Pinchback, T. R.; Clough, S.P.; Heldt, L. A. *Metl. Trans.*, A, **1975**, *6*, 1479: https:// doi. org/10.1007/BF02641959.
7. Misawa,T.; Murakami, H. *Corro. Eng.*, **1976**, *25*(8), 505-507 DOI https://doi .org/ 10. 33 23/jcorr1974.25.8_505.
8. Fouda, A.S.; Ismael, M.A.; Abo Shahba, R.M.; Kamel, L.A.; El-Naggar, A.A. *Int. J. Electrochem. Sci.,* **2017**, *12*, 3361–3384, doi: 10. 20 96 4/2017.04.57.
9. Loto, C.A.;Loto, R.T.;Popoola, A. P. I. *Int. J. Electrochem. Sci.,* **2011**, *6*, 4900-4914.
10. Loto, C.A.; Loto, R.T. Silicon, 2018, https:// doi.org/10.1007/s12633-018-9827-y.
11. Khaled, K.F. *Corro. Sci.*, **2010**, *52*(10), 3225-3234.
12. Zarrouk, B.; Hammouti, H.; Zarrok, M.; Bouachrine, K.F.; Khaled, S.; Al-Deyab, S. *Int. J. Electrochem. Sci.*, **2012**, *7*, 89-105.
13. Barouni, K.; Abdelbaki, K.; Bazzi, L.; Salghi, R; Hammouti, B.; El Issami, S.; Jbara, O.; *Bouachrine. Res. Chem. Intermed.*, **2014**, *40* (3), 991-1002: 10.1007/s11164-012-1016-9.
14. Barouni, K.; Kassale, A.; Albourine, A.; Jbara, O.; Hammouti, B.; Bazzi, L. *Res. Chem. Intermed.*, **2014**, *40*(3), 1016-1019: DOI: 10.1007/s11164-012-1016-9.
15. Ashour, E.A.; Ateya, B. G. *Corro. Sci.*, **1995**, *37*(3), 371-380.
16. Potassium Gluconate, Wikipedia, https:// en.wikipedia.org/wiki/Potassium_gluconate. Accessed: 14 – 09 - 2018.
17. Green Book, 1979, 63, 51 2247, IUPAC Compendium of Chemical Terminology, 2nd ed.
18. Iroha, N.B.; Akaranta, O. James, A.O. Der Chemica Sinica., **2012**, *3*(4), 995-1001.
19. Akalezi, C.O.; Enenebaku, C.K.; Oguzie, E.E. *J. Mater. Environ. Sci.*, **2013**, *4*(2), 217-226.
20. Nnanna, A.L.; Nwadiuko, C.O.;.Ekekwe, D. N; Ukpabi, F. C.; Udensi, C. S.; Okeoma, B.K.; Onwuagba, N.B.; Mejeha, M.I. *Amer. J. Mater. Sci.,* **2011**, *1*(2), 143-148. DOI: 10.5923/j. mate rials. 20110102.24.
21. Santos, A.M.; Almeida, T.F.; Cotting, F.; Aoki, I.V.; Melo, H.G.; Capelossi, V.R. *Mat. Res.*, **2017**, *20*(2), DOI: http://dx.doi. org/10.1590/1980-5373-mr-2016-0963.
22. Ituen, E.B.; Udo, U.E. *Der Chem. Sin.*, **2012**, *3*(6), 1394-1405a.